Kinetic Investigation of the Functional Role of Phenylalanine-31 of Recombinant Human Dihydrofolate Reductase†

Jiu-Tsair Tsay,‡ James R. Appleman,‡ William A. Beard,‡ Neal J. Prendergast,§ Tavner J. Delcamp,§ James H. Freisheim,§ and Raymond L. Blakley*,‡,∥

Department of Biochemical and Clinical Pharmacology, St. Jude Children's Research Hospital, Memphis, Tennessee 38101, Department of Biochemistry, Medical College of Ohio, Toledo, Ohio 43699, and Department of Pharmacology, University of Tennessee College of Medicine, Memphis, Memphis, Tennessee 38163

Received December 27, 1989; Revised Manuscript Received March 26, 1990

ABSTRACT: The role of the active site residue phenylalanine-31 (Phe^{31}) for recombinant human dihydrofolate reductase (rHDHFR) has been probed by comparing the kinetic behavior of wild-type enzyme (wt) with mutant in which Phe^{31} is replaced by leucine (F31L rHDHFR). At pH 7.65 the steady-state k_{cat} is almost doubled, but the rate constant for hydride transfer is decreased to less than half that for wt enzyme, as is the rate of the obligatory isomerization of the substrate complex that precedes hydride transfer. Although steady-state measurements indicated that the mutation causes large increases in K_m for both substrates, dissociation constants for many complexes are decreased. These apparent paradoxes are due to major mutation-induced decreases in rate constants (k_{off}) for dissociation of folate, dihydrofolate, and tetrahydrofolate from all of their complexes. This results in a mechanism proceeding almost entirely by only one of the two pathways used by wt enzyme. Other consequences of these changes are a much altered dependence of steady-state k_{cat} on pH, inhibition rather than activation by tetrahydrofolate, absence of hysteresis in transient-state kinetics, and a decrease in enzyme efficiency under physiological conditions. The results indicate that there is no quantitative correlation between dihydrofolate binding and the rate of hydride transfer for this enzyme.

Dihydrofolate reductase (DHFR)[1] (5,6,7,8-tetrahydrofolate:NADP oxidoreductase, EC 1.5.1.3) catalyzes the NADPH-dependent reduction of 7,8-dihydrofolate (H_2folate) to 5,6,7,8-tetrahydrofolate (H_4folate), an essential cofactor for the biosynthesis of thymidylate and purine nucleotides. The enzyme is the target for a number of antifolate drugs such as methotrexate (MTX) and trimetrexate (anticancer agents), trimethoprim (an antibacterial agent), and pyrimethamine (an antimalarial).

Phenylalanine-31 (Phe^{31}) lies in the entrance to the active site cleft of recombinant human DHFR (rHDHFR) and in the folate complex interacts with both the pteridine moiety and *p*-aminobenzoyl group of the bound folate via hydrophobic contacts (Oefner et al., 1988). However, the Phe^{31} (or Tyr^{31}) side chain in crystal structures of several vertebrate DHFRs has alternate orientations that may be closely related to alternate energetically favored enzyme conformations (Oefner et al., 1988). It was therefore of interest to investigate the role of Phe^{31} by using a mutant of rHDHFR in which Leu replaced Phe^{31} (F31L rHDHFR) that had been produced by oligodeoxynucleotide-directed mutagenesis. The effect of the mutation has been investigated by examining changes in transient- and steady-state kinetics, substrate and product binding, and deuterium isotope effects.

Materials and Methods

Unless otherwise noted the materials and experimental methods used in this study are as previously described (Appleman et al., 1989, 1990), and measurements were made at 20 °C in a buffer mixture (MATS) containing 25 mM MES, 25 mM acetic acid, 50 mM Tris, 100 mM NaCl, and 0.02% sodium azide (pH 7.65). For measurements involving H_4-folate, MATS buffer was supplemented with 50 mM 2-mercaptoethanol. The mutant enzyme, F31L rHDHFR, was prepared by published procedures (Prendergast et al., 1987, 1988). 7,8-Dihydro-L-biopterin (H_2biopterin) was obtained from Dr. B. Schirck's Laboratory (Jona, Switzerland). The concentration of H_2biopterin was determined spectrophotometrically by using a molar extinction coefficient of 10 000 at 280 nm at pH 7.0 (Pfleiderer, 1985).

Dependence of k_{cat} on pH. k_{cat} for F31L enzyme at each pH was determined with NADPH as the variable substrate (5–300 μM) in the presence of 100 μM H_2folate in MATS buffer containing 50 mM 2-mercaptoethanol. The rate was extrapolated to saturating NADPH concentration by fitting the initial rate data to a Michaelis–Menten equation. The pH of the reaction mixture was determined before and after each

† This work was supported in part by U.S. Public Health Service Research Grants RO1 CA 31922 (R.L.B.) and RO1 CA 41461 (J.H.F.), Cancer Core Grant P30 CA 21765 (R.L.B.), and U.S. Public Health Service Training Grant 5 T32 CA 09346 (W.A.B.) from the National Cancer Institute, National Institutes of Health, and by the American Lebanese Syrian Associated Charities (R.L.B., J.-T.T., W.A.B., and J.R.A.).

‡ St. Jude Children's Research Hospital.
§ Medical College of Ohio.
∥ University of Tennessee College of Medicine.

[1] Abbreviations: DHFR, dihydrofolate reductase; rHDHFR, recombinant human DHFR; ECDHFR, DHFR from *Escherichia coli*; H_2-folate, 7,8-dihydrofolate; H_4folate, (6*S*)-5,6,7,8-tetrahydrofolate; H_2biopterin, 7,8-dihydrobiopterin; MATS, 25 mM MES, 25 mM acetate, 50 mM Tris, 100 mM NaCl, and 0.02% sodium azide; MTX, methotrexate; NADPH, nicotinamide adenine dinucleotide phosphate, reduced form; NADP, nicotinamide adenine dinucleotide phosphate, oxidized form; NADPD, (4*R*)-[^{2}H]NADPH; MES, 2-(*N*-morpholino)ethanesulfonic acid; Tris, tris(hydroxymethyl)aminomethane; wt, wild type; F31L, mutant rHDHFR with $Phe^{31} \rightarrow$ Leu; $k_{cat} = V_{max}/[E]$, where V_{max} is the steady-state maximum velocity and [E] is the enzyme concentration.

0006-2960/90/0429-6428$02.50/0

assay. The pH dependence of k_{cat} for F31L rHDHFR was fitted to the equation:

$$k_{cat,app} = \frac{\sigma_1[H^+]^2 + \sigma_2 K_1[H^+]}{[H^+]^2 + K_1[H^+] + K_1K_2} \quad (1)$$

where σ_1 and σ_2 are rate constants and K_1 and K_2 are acid dissociation constants for the diprotonated and monoprotonated species, respectively, and $[H^+]$ is the hydrogen ion concentration.

Product Inhibition. Inhibition of F31L enzyme by NADP was determined with 100 μM H_2folate and 25 μM NADPH and various concentrations of NADP (0–51 μM). The value of K_i was obtained by a nonliner least-squares fit of the initial rate data to the equation for linear competitive inhibition with respect to NADPH. Similarly, the value of K_i for H_4folate was measured in the presence of 8.6 μM H_2folate, 100 μM NADPH, and varying H_4folate concentrations (0–90 μM).

Simulations of the pattern of inhibition by the products using the rate constants in Scheme I indicate that it is linear competitive for H_4folate but is not strictly so for NADP. For this product the pattern of inhibition more closely follows nonlinear competitive kinetics. For this reason, the value of K_i for this product is dependent upon the range of NADP and NADPH concentrations used in the study. Nonetheless, this analysis is useful in elucidating rate constants as described subsequently, and in comparing values of K_i with wt rHDHFR, which also exhibits a complex pattern of inhibition by NADP.

Determination of Association and Dissociation Rate Constants. When data from binding time courses were used, the data were analyzed by equations for second- or pseudo-first-order reactions (Appleman et al., 1988b). The competition method was in general as used previously (Appleman et al., 1988b, 1990). The enzyme concentration was 0.5–3 μM, and the trapping ligand concentration was varied in the range 10–100 μM. The relation between the observed rate constant, k_{obs}, and the concentrations of the dissociating ligand L_1 and the trapping ligand L_2 is

$$k_{obs} = (k_{-1}k_2L_2 + k_{-1}k_{-2} + k_1k_{-2}L_1)/(k_{-1} + k_1L_1 + k_2L_2)$$

where k_1 and k_2 are association rate constants for L_1 and L_2, respectively, and k_{-1} and k_{-2} are corresponding dissociation rate constants. Since in these experiments $k_{-1} \ll k_2L_2 \gg k_{-2}$, this can be simplified to

$$k_{obs} = (k_{-1}k_2L_2 + k_1k_{-2}L_1)/(k_1L_1 + k_2L_2)$$

For different complexes, three types of relations were found between k_{obs} and L_2. In case 1, k_{obs} is independent (or nearly so) of L_2. This results when $k_2L_2 \gg k_1L_1$ and $k_2L_2/k_{-2} \gg k_1L_1/k_{-1}$, so that $k_{obs} = k_{-1}$. This was observed for most complexes. In case 2, k_{obs} is hyperbolically related to L_2 and k_{off} = asymptotic value of k_{obs} at infinite concentration of L_2. This occurs when $k_2L_2/k_{-2} \gg k_1L_1/k_{-1}$, but the condition $k_2L_2 \gg k_1L_1$ is not met. This was observed, for example, for E·NADP with competition by NADPH. k_{-1} can then be obtained from the relation $k_{obs} = k_{-1}L_2/(k_1L_1/k_2 + L_2)$ and an independently determined value of k_2. Values of k_{obs} at various values of L_2 are fitted to the equation by a nonlinear least-squares technique. The fit gives values of both k_1 and k_{-1}. In practice all data for apparent case 1 complexes were also treated in this way. In case 3, k_{obs} is linearly related to $1/L_2$ with $k_{off} = k_{obs}$ at the ordinate intercept. This corresponds to the situation where $k_2L_2 \gg k_1L_1$, but the condition $k_2L_2/k_{-2} \gg k_1L_1/k_{-1}$ is not met, so that $k_{obs} = k_{-1} + k_{-2}k_1L_1/k_2L_2$. This was observed for E·NADPH with NADP as the competing ligand.

Table I: Michaelis Constants and Steady-State Rates for the Dihydrofolate Reduction Catalyzed by Wild-Type and F31L rHDHFR

	K_m (μM)		
	H_2folate	NADPH	k_{cat}[a] (s^{-1})
F31L	0.77 ± 0.11	21.9 ± 1.2	22.2 ± 0.4
wt[b]	0.1 ± 0.03	0.16 ± 0.06 4.2 ± 2.3	12.5 ± 0.2
ratio F31L/wt	7.7	137 5.2	1.8

[a] $k_{cat} = V_{max}/[E]$. [b] Values for wt enzyme are taken from Appleman et al. (1990).

Where there is strong negative cooperativity for ligand binding in a ternary complex (as encountered for the F31L DHFR complex with NADPH and H_4folate), measurement of k_{off} for one ligand (H_4folate) by competition by a trapping ligand (MTX) may be complicated by difficulty in saturating the enzyme with the second ligand of the ternary complex (in this case, NADPH). In such a case the k_{off} calculated for a fixed concentration of the two ligands and a series of concentrations of the trapping ligand is an apparent value. A series of these values at different concentrations of the second ligand (NADPH), and with the use of a large excess of the trapping ligand (MTX) over the ligand it is displacing (H_4-folate), gives a hyperbolic relation of apparent k_{off} and [NADPH] from which the true k_{off} is computed by fitting to the equation $k_{obs} = (k_{off}[NADPH] + k'_{off}K_d)/(K_d + [NADPH])$, where k_{off} is the rate constant for H_4folate release from the E·H_4folate·NADPH complex, K_d is the apparent dissociation constant for NADPH for this complex, and k'_{off} is the previously determined rate constant for H_4folate release from the E·H_4folate complex.

Progress Curves for F31L rHDHFR Catalyzed Reduction of H_2folate by NADPH. Time courses of product formation were measured as described previously (Appleman et al., 1990) from the decrease in absorbance at 340 nm accompanying conversion of NADPH and H_2folate to NADP and H_4folate.

Simulation of Catalytic Behavior from Rate Constants. Simulations of the time courses of catalytic reactions and the dependence of the catalytic rate on the concentrations of substrates and products were carried out by using the modified computer program CRICF (Appleman et al., 1990).

Results

Steady-State Parameters and pH Dependence of k_{cat}. At pH 7.65 k_{cat} and K_m for both substrates are significantly greater for F31L rHDHFR than for wild-type enzyme (Table I). The Lineweaver–Burk plots of $1/k_{cat}$ vs $1/[S]$ for H_2folate and NADPH with F31L enzyme are linear (Figure 1), so that F31L enzyme exhibits only a single K_m for NADPH or for H_2folate, in contrast to the two K_m values for NADPH found with wt rHDHFR (Appleman et al., 1990). F31L enzyme is inhibited by the reaction products NADP and H_4folate (Figure 2). When K_m values of 21.9 μM and 0.77 μM are used for NADPH and H_2folate, respectively, K_i values of 8.2 ± 0.5 for NADP and 2.4 ± 0.1 μM for H_4folate were computed by nonlinear least-squares fit of the data to a hyperbolic inhibition curve. For wt rHDHFR K_i for NADP is 0.21 μM, but H_4folate activates the wt enzyme (Appleman et al., 1990).

k_{cat} for wt rHDHFR is relatively pH-independent in the range of 6–9 (Figure 3A) but increases at pH 5 and decreases at pH 10. However, the pH dependence of k_{cat} for F31L rHDHFR is bell-shaped, indicating effects by two protonations. Fitting of the data to the appropriate equation, as described under Materials and Methods, gave 4.7 ± 1.2 s^{-1} and 25.6 ± 1.8 s^{-1} for k_{cat} of the diprotonated and mono-

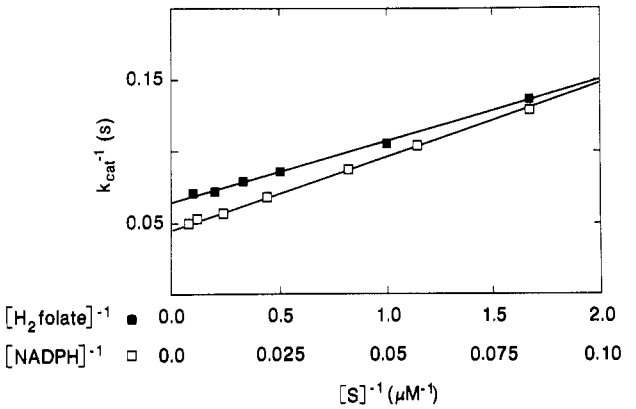

FIGURE 1: Lineweaver–Burk plot of $1/k_{cat}$ vs $1/[S]$ for F31L rHDHFR catalyzed reduction of H_2folate by NADPH. Initial rate assays were performed as described under Materials and Methods either with H_2folate (■) as a variable substrate in the presence of 100 μM NADPH or with NADPH (□) as a variable substrate in the presence of 100 μM H_2folate. Solid lines represent the computed best fit of the data to the Michaelis–Menten equation.

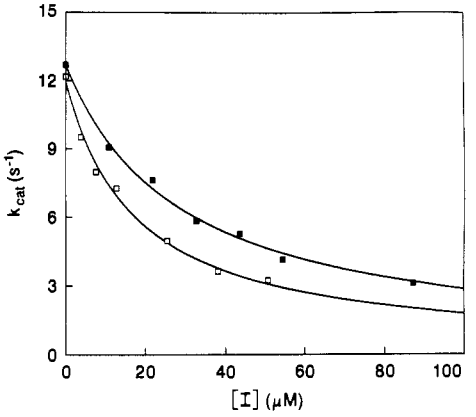

FIGURE 2: Inhibition of F31L rHDHFR by products. Initial rates (over 3 min) were measured at the indicated concentrations of NADP (□) or H_4folate (■) and with 1 nM F31L rHDHFR. Other concentrations were as follows: for NADP inhibition, 100 μM H_2folate and 25 μM NADPH; for H_4folate inhibition, 8.6 μM H_2folate and 100 μM NADPH. The solid curve represents the best fit of the data.

protonated species, respectively. At high pH (unprotonated species) k_{cat} approaches zero. The calculated acid dissociation constants, pK_1 and pK_2, are 6.8 ± 0.2 and 9.0 ± 0.1. The decrease in k_{cat} at high pH is due to the decreased rate of hydride transfer which contributes to rate limitation above pH 8 as shown by $^Dk_{cat}$ values (Figure 3B). At pH <7 some other process becomes rate limiting, possibly H_4folate dissociation from F31L·NADPH·H_4folate since this k_{off} is much lower than for dissociation for the similar complex of wt enzyme.

Values of the steady-state kinetic constants obtained in this study are significantly higher than those we reported previously for F31L enzyme (Prendergast et al., 1989). The cause of this discrepancy is the considerable difference in buffer composition, particularly the higher ionic strength used in the present study, which has a marked effect on ligand dissociation from complexes. The MATS buffer system used herein was chosen to ensure constant ionic strength over the range of pH employed in this study, and the higher ionic strength (150 mM) more closely corresponds to physiological conditions. Nonetheless, the conclusions drawn on the basis of experiments reported in the previous publication remain valid, and the current work represents a significant extension of our previous studies.

Effect of the Phe^{31} → Leu Mutation on Hydride Transfer. The increased k_{cat} suggests greater catalytic efficiency for the

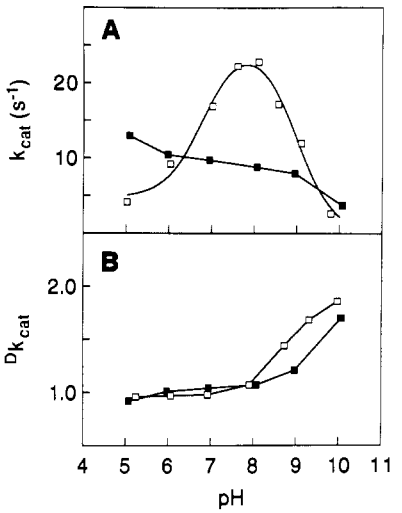

FIGURE 3: Variation of k_{cat} and $^Dk_{cat}$ with pH. Panel A: pH dependence of k_{cat} (s^{-1}) for wt (■) and k_{cat} for F31L rHDHFR (□). k_{cat} for wt enzyme was measured at saturating conditions (200 μM substrates). k_{cat} for F31L enzyme was determined with NADPH as the variable substrate in the presence of 100 μM H_2folate and was calculated by fitting the data to the Michaelis–Menten equation. The solid line of the bell-shaped curve for F31L enzyme is a fit to eq 1 as described under Materials and Methods. Panel B: pH dependence of $^Dk_{cat}$ for wild type (■) and for F31L rHDHFR (□). $^Dk_{cat}$ = k_{cat}(NADPH)/k_{cat}(NADPD).

Table II: Observed Transient-State Kinetics and Rate Constant for Hydride Transfer for rHDHFR[a]

enzyme	k_b (s^{-1})	^Dk_b	k_0 (s^{-1})	k_1 (s^{-1})
F31L[b]	520	1.9	675	1200
wt[c]	600	2.1	2200	3000

[a] Determinations were conducted with 15 μM wt and 3 μM F31L rHDHFR and 100 μM substrates. k_b is the corrected rate constant for transient kinetics of product formation. ^Dk_b = k_b(NADPH)/k_b(NADPD). k_0 is the rate constant for the obligatory isomerization of the ternary substrate complex. k_1 is the rate constant for hydride transfer. Values for k_0 and k_1 were determined from k_b and ^Dk_b and a correction curve as described by Beard et al. (1989). [b] Values for F31L enzyme were measured at 20 °C. [c] Values for wt rHDHFR were taken from Beard et al. (1989). k_b and ^Dk_b were measured at 6 °C, and values of k_0 and k_1 are corrected to 20 °C.

mutant enzyme, and it was therefore of interest to determine the effect of the mutation on the rate of hydride transfer. However, a complication in this determination is that for DHFR from many sources the reaction rate in the exponential burst phase is limited not only by hydride transfer between enzyme-bound substrates but also partly by an obligatory isomerization of the ternary substrate complex (Beard et al., 1989). This follows from an observed isotope effect for the burst phase, ^Dk_b, considerably lower than the value expected for hydride transfer (Beard et al., 1989). From the measured ^Dk_b and an assumed isotope effect of 3.4 for hydride transfer (Beard et al., 1989), rate constants for hydride transfer and for isomerization can be calculated (Table II). Although the rate of product formation at pH 7.65 by F31L enzyme during the burst phase is very rapid, 520 s^{-1} at 20 °C, it is considerably slower than for wt (600 s^{-1} at 6 °C corresponding to 1360 s^{-1} at 20 °C). The rate constants for both hydride transfer and isomerization are significantly lower for F31L enzyme than for wt, but much higher than k_{cat}, the steady-state rate of product formation, so that neither hydride transfer nor the isomerization contributes significantly to limitation of k_{cat} at this pH.

pH Dependence of $^Dk_{cat}$. In order to confirm that some step other than hydride transfer is rate limiting during steady state

Table III: Association Rate Constants for Ligand Binding to Wild-Type and F31L rHDHFR[a]

ligand	form of enzyme combining	$k_{on} \times 10^{-6}$ (M^{-1} s^{-1}) F31L	wt[b]	ratio F31L/wt
folate	E	55.0 ± 0.3	156	0.35
	E·NADPH	24.7 ± 0.3	58	0.43
H_2folate	E	96.8 ± 0.8	264	0.37
	E·NADPH[c]	33.7 ± 0.6	98	0.34
	E·NADP	23.6 ± 0.4	110	0.22
H_4folate	E	61.6 ± 0.4	117	0.53
	E·NADPH	13.8 ± 0.1	14	0.99
	E·NADP	8.2 ± 0.1	24	0.34
NADPH	E	35.0 ± 0.3	38	0.92
	E·H_2folate[c]	27.9 ± 0.4	24	1.16
	E·H_4folate	4.6 ± 0.2	4.4	1.05
NADP	E	16.4 ± 0.4	17	0.96
	E·H_2folate	20.0 ± 0.2	20	1.0
	E·H_4folate	0.39 ± 0.04	0.7	0.56

[a] Except where noted, these values were calculated as described under Materials and Methods from time courses of fluorescence transients accompanying ligand binding. [b] Values for wild-type rHDHFR are taken from Appleman et al. (1990). [c] From the time course of the burst of product formation.

Table IV: Dissociation Rate Constants Obtained by the Relaxation Method for Wild-Type and F31L rHDHFR Complexes[a]

ligand	enzyme complex dissociating	k_{off} (s^{-1}) F31L	wt[b]	ratio F31L/wt
folate	E·folate	1.8 ± 0.06	27	0.067
	E·NADPH·folate	0.8 ± 0.1	88	0.009
H_2folate	E·H_2folate	8.7 ± 0.4	12	0.73
	E·NADPH·H_2folate	2.65[c]	94[c]	0.028
	E·NADP·H_2folate	≪1	1.3	≪0.77
H_4folate	E·H_4folate	3.4 ± 0.3	5.4	0.67
	E·NADP·H_4folate	4.5 ± 0.1	63	0.41
NADPH	E·NADPH	3.1 ± 0.2	1.3	2.4
	E·H_2folate·NADPH	160[c]	19[c]	8.4
	E·H_4folate·NADPH	100 ± 10	100[d]	1.0
NADP	E·NADP	32.1 ± 1.7	35.6	0.90
	E·H_2folate·NADP	2.3 ± 0.2	4.6	0.50
	E·H_4folate·NADP	135 ± 7	96	1.4

[a] Except where noted, these values were calculated as described under Materials and Methods from time courses of fluorescence transients accompanying ligand binding. [b] Values for wild-type rHDHFR are taken from Appleman et al. (1990). [c] Estimated by simulation, as described under Materials and Methods. [d] Determined by the competition method.

at pH 7.65, we examined the isotope effect on k_{cat} at this and other pH values. $^{D}k_{cat}$ is the ratio of k_{cat} with NADPH as substrate to k_{cat} with NADPD. With saturating concentrations of H_2folate and NADPH or NADPD, $^{D}k_{cat}$ was close to 1.0 over the pH range 5–8 for both enzymes (Figure 3B). Above pH 8 $^{D}k_{cat}$ for F31L is higher than that for wt enzyme, but the values of $^{D}k_{cat}$ for both enzymes increase in a parallel fashion as the pH increases. If the intrinsic deuterium isotope effect on the rate of hydride transfer is 3.4 as observed for DHFR from some sources (Beard et al., 1989), it is clear that hydride transfer is rate limiting for neither F31L nor wt rHDHFR below pH 8 and is only partially rate limiting above this pH.

Association and Dissociation Rate Constants from Transient-State Kinetics. In order to understand the changes in steady-state kinetics induced by the mutation, it was necessary to determine the effect of the mutation on the various association and dissociation rate constants for all the complexes of substrates and ligands with the enzyme. Association and dissociation rate constants (k_{on} and k_{off}, respectively) were determined from the transient-state kinetics of substrate and product binding to form binary and ternary complexes with

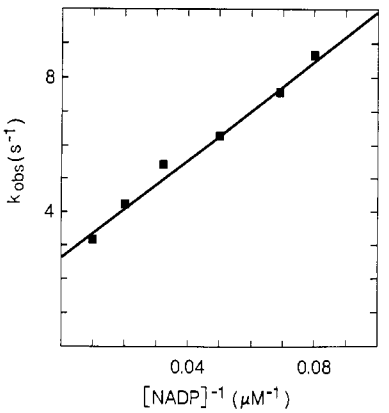

FIGURE 4: Dependence of the apparent first-order rate constant (k_{obs}) on reciprocal NADP concentration in the displacement of NADPH from E·NADPH complex by NADP. The final concentrations of F31L rHDHFR and NADPH were 0.5 and 2.5 μM, respectively. The concentration of NADP was varied from 10 to 100 μM.

F31L enzyme (Tables III and IV). k_{on} values for formation of binary or ternary complexes of folate, H_2folate, and H_4folate are decreased by a factor of 0.2–0.6 compared with wt enzyme (Table III) except that k_{on} for H_4folate binding to F31L·NADPH is unaltered. k_{on} values for NADPH and NADP are comparable for the two enzymes (Table III). The standard errors given for the low k_{off} values in Table IV are considerably underestimated by the program used to fit the data to the second-order reaction equation. This was indicated by the fact that the fit of the data to the computed curve was little changed when the value of k_{off} was fixed at alternative widely divergent values.

Equilibrium between Apoenzyme Conformers. In the formation of binary complexes of F31L rHDHFR with NADPH or with NADP, the time course of fluorescence change was governed by two exponentials: a rapid phase dependent on ligand concentration (giving the values of k_{on} and k_{off} in Tables III and IV, respectively), followed by a slow phase independent of ligand concentration. The values of k_{obs} for the slow phase of NADPH and NADP binding to enzyme are 0.11 ± 0.002 and 0.12 ± 0.003 s^{-1}, respectively. This biphasic behavior has been observed for binding of nucleotides to *Escherichia coli* DHFR (ECDHFR) (Cayley et al., 1981) and wt rHDHFR (Appleman et al., 1990) and has been attributed to rapid binding of nucleotide to only one of two enzyme conformers. The equilibrium constant governing distribution of enzyme between these conformers can be determined from the ratio of the amplitudes of the fast and slow phases. Eighty percent of the enzyme was present as the conformer binding nucleotide, the same proportion observed for the wt enzyme (Appleman et al., 1990).

Dissociation Rate Constants by the Competition Method. As previously noted, many of the dissociation rate constants obtained by analysis of the transient-state kinetics of ligand binding (relaxation method) shown in Table IV are subject to much larger errors than the table indicates. Relaxation values of dissociation rate constants are often overestimates, especially if k_{off} is small. Fortunately, in many cases k_{off} can also be measured by competition experiments in which the ligand initially bound is displaced by a second ligand that binds at the same site (Birdsall et al., 1980). However, as discussed under Materials and Methods, the observed rate constant is not always identical with k_{off}, and the relation between k_{obs} and the trapping ligand concentration was investigated in order to obtain a true value of k_{off}. Figure 4 shows that the plot of k_{obs} versus reciprocal NADP concentration is linear in the competition of NADPH from its binary complex, and the

Table V: Dissociation Rate Constants from Competition Experiments

released ligand	enzyme complex dissociating	trapping ligand	k_{off} (s^{-1}) F31L	k_{off} (s^{-1}) wt	ratio F31L/wt
folate	E·folate[a]	MTX	0.37 ± 0.004	25	0.015
	E·NADPH·folate[c]	MTX	0.28 ± 0.003	70	0.004
H_2folate	E·H_2folate[a]	MTX	0.12 ± 0.001	14	0.01
	E·NADP·H_2folate[b]	MTX	(2.8 ± 0.06) × 10^{-3}	1.3	0.002
H_4folate	E·H_4folate[a]	MTX	0.15 ± 0.001	5.1	0.03
	E·NADPH·H_4folate[c]	MTX	29.8 ± 0.7	225	0.13
	E·NADP·H_4folate[b]	MTX	1.00 ± 0.02	46	0.02
NADPH	E·NADPH[d]	NADP	3.2 ± 0.2	1.7	1.9
NADP	E·NADP[e]	NADPH	25.7 ± 0.05	32	0.8
	E·H_2folate·NADP[f]	NADPH	2.1 ± 0.02	4.6	0.46

[a] Quenching of protein fluorescence below 360 nm as MTX displaced H_2folate. [b] Increase in absorbance at 340 nm accompanying protonation of MTX upon binding to F31L rHDHFR. [c] Decrease in absorbance at 380 nm accompanying protonation of MTX upon binding to F31L rHDHFR with varying NADPH concentrations. [d] Decrease in fluorescence intensity above 380 nm as NADP displaces NADPH. [e] Increase in fluorescence intensity above 380 nm as NADPH displaces NADP. [f] Decrease in absorbance at 340 nm due to reaction as NADPH replaces NADP.

Table VI: Comparison of Equilibrium and Kinetic Dissociation Constants for Binary and Ternary Complexes of F31L rHDHFR[a]

enzyme complex	dissociating ligand	F31L K_D[b]	F31L % quench	F31L k_{off}/k_{on}[c]	wt K_D[d]	wt k_{off}/k_{on}[d]
E·folate	folate	10 ± 2	92	6.7 ± 0.1	83	173
E·NADPH·folate				11.3 ± 0.2		1 210
E·H_2folate	H_2folate	1.8 ± 1.7	95	1.2 ± 0.01	120	53
E·NADP·H_2folate		3.3 ± 2.2	84	0.12 ± 0.04		12
E·NADPH·H_2folate				79 ± 2		960
E·H_4folate	H_4folate	2.7 ± 1.3	82	2.4 ± 0.02	50	44
E·NADPH·H_4folate				2 160 ± 70		16 100
E·NADP·H_4folate				122 ± 3		1 920
E·NADPH	NADPH	35 ± 6	82	91 ± 6	50	45
E·H_4folate·NADPH				21 740 ± 2 370		22 700
E·H_2folate·NADPH				5 730 ± 80		790
E·NADP	NADP	1200 ± 100	75	1 585 ± 40	2300	1 880
E·H_2folate·NADP				105 ± 1		230
E·H_4folate·NADP				346 000 ± 40 000		120 000

[a] All values are in nanomolar (nM). [b] By fluorescence titration. With the instrumentation employed in this study, K_D values less than 5 nM were difficult to measure and suffered from large standard deviations. [c] Values of k_{on} are from Table III. k_{off} values are from Table V where available; otherwise, they are from Table IV. [d] Values of K_D and k_{off}/k_{on} for wt rHDHFR from Appleman et al. (1990). Values of k_{off} are from the competition method where available.

ordinate intercept gives the true k_{off}. On the other hand, k_{obs} for release of NADP from its binary complex with F31L enzyme was hyperbolically related to the concentration of NADPH, the displacing ligand (data not shown), and the true k_{off} was the asymptotic value of k_{obs} at saturating NADPH.

Where there is large negative cooperativity between ligands forming a ternary complex, this necessitates a different type of competition experiment in which k_{obs} must be obtained at a series of concentrations of the second ligand (see Materials and Methods). This was the case for k_{off} for H_4folate from the abortive complex F31L·NADPH·H_4folate. Figure 5 shows that k_{obs} increases hyperbolically with increasing NADPH concentration, and the true value of k_{off} for H_4folate is the asymptotic value of k_{obs} at saturating NADPH. Dissociation rate constants determined by competition experiments are recorded in Table V.

Relaxation values of k_{off} obtained by transient-state kinetics of binding (Table IV) and competition techniques (Table V) are identical for many complexes of wt enzyme. Although these two methods give similar k_{off} values for complexes of NADPH and NADP with F31L enzyme, apparently higher values were obtained by the relaxation method for complexes of folate, H_2folate, and H_4folate with mutant enzyme (Tables IV and V), but it is uncertain whether this apparent divergence is significant.

Equilibrium Dissociation Constants from Fluorescence Titration. The dissociation constant (K_D) for equilibrium binding of folates or nucleotides of F31L rHDHFR was determined by measuring either the concomitant decrease in enzyme fluorescence or the increase in bound NADPH fluorescence through energy transfer. Titration values of K_D for various binary complexes and one ternary complex are given in Table VI, together with kinetically determined values. At equilibrium, F31L enzyme binds H_2folate and H_4folate with high and nearly equal affinity in the low nanomolar ranges. Nucleotides bind to both enzymes similarly, with NADP binding much more weakly than NADPH.

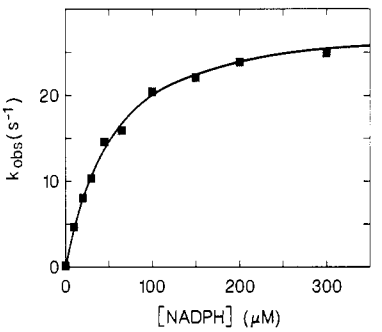

FIGURE 5: Dependence on NADPH concentrations of the apparent first-order rate constant (k_{obs}) for H_4folate release from the abortive complex F31L·NADPH·H_4folate. MTX was used as competing ligand. Final concentrations were as follows: F31L rHDHFR, 2 μM; H_4folate, 3 μM; and MTX, 50 μM. The best fit line was calculated as described under Materials and Methods.

Rate Constants for the Ternary Substrate Complex and Simulation of Steady-State Kinetics. Association rate constants for binding H_2folate to E·NADPH or NADPH to E·H_2folate to form the reactive ternary complex E·

Scheme I: Kinetic Scheme for F31L rHDHFR at 20 °C and pH 7.65[a]

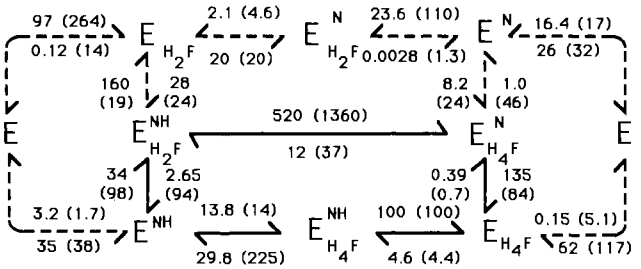

[a] E = rHDHFR, NH = NADPH, H_2F = H_2folate, N = NADP, and H_4F = H_4folate. Values of k_{off} (in units of s^{-1}) are from Table V except in two cases. The remaining values of k_{off} and all values of k_{on} (in units of μM^{-1} s^{-1}) are from Table IV and III, respectively. Rate constants for interconversion of ternary substrate and ternary product complexes were determined as described under Materials and Methods. The major steps in the catalytic cycle at steady state in the presence of saturating substrate concentrations are depicted by the cycle of bold solid arrows. Broken arrows indicate pathways of minor significance at steady state. Values in parentheses are for wt enzyme; those without parentheses are for the F31L mutant enzyme.

NADPH·H_2folate were measured in single-turnover experiments under conditions where formation of the substrate ternary complex was slower than conversion of the substrate complex to the product complex (Table III). However, dissociation rate constants for this complex are difficult to measure directly because of the high rate of chemical transformation of E·NADPH·H_2folate to E·NADP·H_4folate. Instead, k_{off} was obtained by computer simulation of steady-state behavior of the mutant enzyme. The association and dissociation rate constants from Tables III to V were entered into a scheme showing all possible interconversions of enzyme forms (Scheme I). It is evident from relative values of rate constants that the observed inhibition of activity by NADP must be due primarily to competition of NADP and NADPH for binding to E·H_2folate. Although the latter is not an intermediate in the preferred pathway at steady state (lower cycle with bold arrows), it can be formed by dissociation of NADPH from the substrate ternary complex. Consequently, the rate of such NADPH dissociation markedly affects the extent of NADP inhibition. A modification of the computer program CRICF (Appleman et al., 1990) was used to simulate NADP inhibition as measured by initial steady-state rates of product formation. In these simulations various values of k_{off} for NADPH from E·NADPH·H_2folate were combined with other rate constants in Scheme I. The best fit value of k_{off} for NADPH was 160 s^{-1}. k_{off} for H_2folate from the E·H_2folate·NADPH complex was then chosen to balance the binding equilibria within the E, E·NADPH, E·H_2folate, and E·NADPH·H_2folate system, and a value of 2.65 s^{-1} was obtained.

With these values, simulation gave the following kinetic parameters: with 100 μM NADPH and H_2folate varied, k_{cat} = 18.3 ± 0.04 s^{-1}, K_m = 0.53 ± 0.004 μM; with 100 μM H_2folate and NADPH varied, k_{cat} = 21.7 ± 0.04 s^{-1}. It may be seen that agreement with observed values (Table I) is good. This model also predicts K_i for H_4folate of 2.5 ± 0.01 μM in agreement with the observed value. Note that the experimental value of K_m for NADPH was used in calculating k_{off} and k_{on} for both ligands in the E·NADPH·H_4folate complex, and the experimental value of K_i for NADP was used to calculate k_{off} for NADPH from the E·H_2folate·NADPH complex. The agreement between calculated and experimental values of K_m for NADPH and K_i for NADP is therefore not a test of the model. Figure 6 shows the full time courses of product formation for F31L rHDHFR catalyzed reduction of

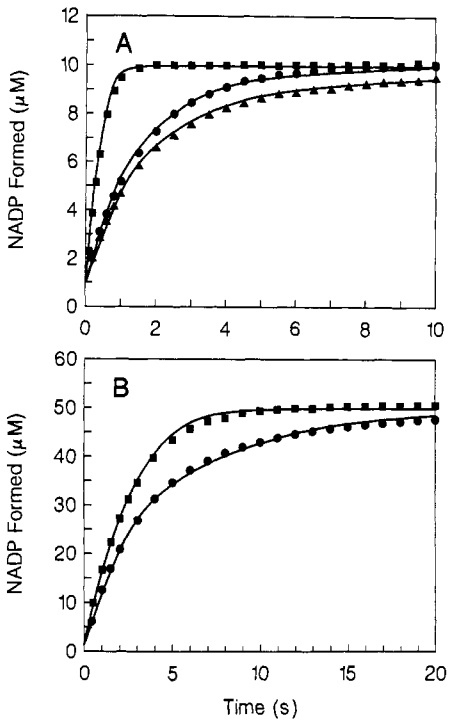

FIGURE 6: Complete time courses for the reduction of H_2folate by NADPH catalyzed by F31L rHDHFR. The solid lines are simulations from the model and rate constants in Scheme I. For simplicity only some of the experimental data points are presented. The concentration of F31L rHDHFR was 1 μM. The concentrations of NADPH and H_2folate, respectively, were as follows: in panel A, 100 and 10 μM (■), 10 and 100 μM (●), and 10 and 10 (▲); in panel B, 100 and 50 μM (■) and 50 and 100 μM (●).

H_2folate by NADPH with diverse combinations of substrate concentrations, as measured in the stopped-flow spectrophotometer (for simplicity only selected data points are shown). The solid lines are simulated progress curves, each corresponding to one set of experimental conditions. The fit to the corresponding experimental data is excellent in all cases.

A deficiency of the model shown in Scheme I is that there is poor agreement between estimates of the thermodynamic equilibria obtained from alternate pathways between the same intermediates. This discrepancy probably arises from two sources. One is experimental errors in the determination of one or more of the rate constants in the scheme. The other is the occurrence of rapid conformational isomerizations of some of the complexes of H_2folate and H_4folate, evidence for which will be presented in another publication. These isomerizations would cause marked changes in the dissociation constants for ligands from values for the initial complexes to the values that are obtained by measuring k_{off} in competition experiments. However, the former would not be appropriate during the operation of the complete catalytic cycle of reactions, and since the ratio of k_{off} by competition to k_{on} does not necessarily equal the thermodynamic K_D when isomerization occurs (Appleman et al., 1988a), the thermodynamic equilibria cannot be calculated from the latter.

Binding of H_2biopterin to Wild-Type and Mutant rHDHFR. The dissociation constants for H_2biopterin to wt and to F31L rHDHFR apoenzyme, determined by fluorescence titration, indicated that binding to the two enzymes is similar and very weak (Table VII). Measurements of k_{on} for H_2biopterin could not be determined directly by measurement of fluorescence changes because binding is weak, k_{off} is large, and the requisite concentration of ligand gave very large inner-filter effects. Both k_{on} and k_{off} for the binary complex were determined by competition experiments in which MTX dis-

Table VII: Association and Dissociation Rate Constants and Equilibrium Dissociation Constant for H_2biopterin Binding to Wild-Type and F31L rHDHFR[a]

	wt	F31L	ratio wt/F31L
$k_{on} \times 10^{-6}$ (M^{-1} s^{-1})	40 ± 16	13 ± 2	3.1 ± 1.3
k_{off} (s^{-1})	2045 ± 532	405 ± 36	5.0 ± 1.4
k_{off}/k_{on} (μM)	51 ± 24	31 ± 5	1.6 ± 0.8
K_D (μM)	31 ± 5	28 ± 5	1.1 ± 0.3

[a] Values of k_{on} and k_{off} were calculated as described under Materials and Methods from competition experiments. Values of K_D were determined by fluorescence titration.

placed H_2biopterin (see Materials and Methods under case 2 for competition). As seen in Table VII, the mutation decreases k_{on} and k_{off} by small and similar factors.

Discussion

Effects of the Mutation on Ligand Binding. An X-ray diffraction model for an HDHFR–NADPH complex has yet to be reported, so that it is unknown whether interaction of Phe[31] with the nicotinamide moiety of bound NADPH occurs. Although Oefner et al. (1988) published a stereo diagram of HDHFR with NADPH modeled in the active site of the rHDHFR·folate complex some time ago, they have not made atomic coordinates for this model available, so that it is unknown whether the model predicts such direct interaction. The Phe[31] → Leu mutation has little effect on k_{on} for NADP and NADPH (Table III), and the only increase in k_{off} is for NADPH dissociation from the substrate ternary complex, but this value is derived indirectly and is subject to greater error. A lack of major effects of the mutation on the association and dissociation of NADPH and NADP is consistent with an absence of direct interaction of Phe[31] with these ligands.

The diagrams of Oefner et al. (1988) appear to indicate hydrophobic interaction of Phe[31] with the pteridine ring of bound folate in the complex with rHDHFR. Replacing Phe[31] with the smaller Leu causes small decreases in the rate of combination of the pteridine substrates with the enzyme (Table III), which is consistent with such an interaction. However, contrary to expectation, values of k_{off} for pteridine substrates are much lower than for wt enzyme (Table V).

As might be anticipated, ligand binding is decreased by most of the mutations at the active site of DHFR that have been investigated (Chen et al., 1985; Mayer et al., 1986; Chen et al., 1987; Howell et al., 1987; Benkovic et al., 1988; Thillet et al., 1988; Taira & Benkovic, 1988; Murphy & Benkovic, 1989). The Phe[31] → Leu mutation in rHDHFR was the first case reported (Prendergast et al., 1989) in which the replacement *increased* binding of folate, H_2folate, and H_4folate. Shortly thereafter, Schweitzer et al. (1989) reported that the Phe[31] → Ser mutation also increases the binding of H_2folate. However, these Phe[31] mutations differ in their effects on MTX binding since compared with wt the dissociation constant is *decreased* slightly for the F31L enzyme (Prendergast et al., 1989) but *increased* 100-fold for the F31S mutant. Results with the Phe[31] mutants therefore indicate that although the area and contour of the hydrophobic active site surface may be a factor influencing catalytic efficiency (Benkovic et al., 1988), there are other important influences. The decreased rate of hydride transfer and increased H_2folate binding in the F31L enzyme is a second example [cf. Murphy and Benkovic (1989)] of the disconnection between these functional parameters of DHFR, which earlier had seemed to be closely linked (Benkovic et al., 1988).

The increased binding of the pteridines is perhaps due to inclusion of an additional bound water molecule in the binding cavity of the mutant enzyme, or to changes in side-chain orientations that may permit new direct or indirect interactions of bound ligand with the enzyme. Another possibility, however, is that after formation of the initial complexes with the mutant enzyme by these ligands, a conformational change occurs which prevents dissociation of substrate unless the change is reversed. This conformational isomerization must be forbidden in the wt enzyme. Evidence of such an isomerization of the MTX complex has been reported previously (Appleman et al., 1988b). Evidence for isomerization of complexes of F31L rHDHFR with folates will be presented in another publication. It is perhaps significant that binding of H_2biopterin, a weakly bound alternate substrate, is not affected appreciably by the Phe[31] → Leu mutation (Table VII). This substrate has an L-*erythro*-dihydroxypropyl side chain instead of the [4-(methylamino)benzoyl]glutamate side chain of the folates. The larger side chain therefore seems to be necessary for the isomerization of the complex.

Effect of the Mutation on the Catalytic Cycle. As may be seen from the rate constants in Scheme I, NADP dissociates from the ternary product complex of F31L enzyme 135 times faster than H_4folate at pH 7.65, so that the cycle proceeds via the enzyme·H_4folate complex. Direct dissociation of H_4folate from this complex is very slow, however, and is preceded by binding of NADPH. The negative cooperativity in this binding increases the rate of dissociation of H_4folate 200-fold (k_{off} 29.8 s^{-1}). Finally, H_2folate binds to the enzyme·NADPH complex to give the substrate ternary complex. Relatively little reaction occurs by the alternate upper pathway involving enzyme·NADP. This is in contrast to wt enzyme, which utilizes the lower pathway via enzyme·H_4folate for the first few cycles but at steady state accumulates predominantly in the upper pathway involving enzyme·NADP. Consequently, at steady state the two enzymes have different rate-limiting steps. For wt it is mainly dissociation of NADP from the enzyme·H_2folate·NADP complex, whereas for F31L enzyme the major limitation is the rate of dissociation of H_4folate from enzyme·H_4folate·NADPH with some contribution also by the dissociation of NADP from the ternary product complex. Reaction through pathways involving apoenzyme, commonly assumed in schemes based on steady-state kinetics, is negligible for either enzyme. The different mechanisms for the wt and mutant enzymes are reflected in the calculated concentrations of enzyme complexes present at steady state in the presence of saturating concentrations of substrates (Figure 7A). The high proportion of E·NADP·H_2folate for wt enzyme and of E·NADPH·H_4folate for the mutant enzyme are particularly significant. It should be noted, however, that these distinctions are less marked under conditions approximating those in a eukaryotic cell (Figure 7B).

Effect of the Changed Pathway on Steady-State Kinetics. The different mechanistic pathway followed by the mutant enzyme accounts for the changes in steady-state behavior caused by the mutation. These are as follows: higher k_{cat} at pH 7.65; changed k_{cat} dependence on pH; higher K_m for both substrates; higher K_i for NADP; and inhibition rather than activation by H_4folate. The higher k_{cat} is due to the change in the rate-limiting step and the fact that in this step H_4folate dissociation from its complex with F31L·NADPH (k_{off} 29.8 s^{-1}) is faster than NADP release from its complex with wt·H_2folate (k_{off} 4.6 s^{-1}).

Although the inhibition by NADP is weaker for F31L (K_i 8.2 μM) than for wt enzyme (K_i 0.2 μM), it is nevertheless substantial and is due to a small amount of enzyme cycling through the E·NADP, E·NADP·H_2folate pathway. For wt

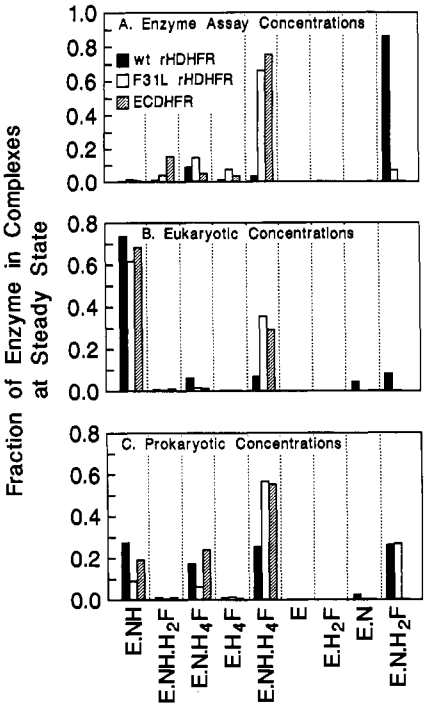

FIGURE 7: Distribution of F31L and wt rHDHFR and ECDHFR among enzyme complexes at steady state (1 min after mixing) computed from rate constants in Scheme I. Changes from the initial concentrations over this time period were assumed negligible. Concentrations and values of pH were as follows: (A) 250 μM NADPH and 50 μM H_2folate at pH 7.65; (B) 2000 μM NADPH, 0.1 μM H_2folate, 20 μM NADP, and 1 μM H_4folate at pH 7.0; (C) 1000 μM NADPH, 0.3 μM H_2folate, 1500 μM NADP, and 13 μM H_4folate at pH 7.0. Concentrations were chosen as described previously to be representative of eukaryotic cells in (B) (Appleman et al., 1990) and of prokaryotic cells in (C) (Benkovic et al., 1988). For wt and F31L rHDHFR, it was assumed that all rate constants are pH-independent. Although the rate of hydride transfer is anticipated to be faster at pH 7.0 than at pH 7.65 for these enzymes, the rate of conversion of enzyme-bound substrates to products is primarily limited by an isomerization of the ternary substrate complex, which may be pH-independent. Rate constants used in the computation of the distribution of complexes of ECDHFR were taken from Fierke et al. (1987). Since constants in this latter group were determined at 25 °C rather than at 20 °C like those for rHDHFRs, they were corrected to 20 by assuming that the Q_{10} equals 2 (activation energy = 11.8 kcal/mol). Also, the rate of hydride transfer for ECDHFR was assumed to follow the pH dependence described by Fierke et al.

enzyme H_4folate increases the steady-state rate because it directs more reaction through the lower, faster cycle at the expense of the upper enzyme·H_2folate·NADP route. Such activation does not occur with F31L enzyme because at steady state there is negligible flow through the upper pathway.

As reported under Results, the mechanistic model proposed and the value of rate constants shown in Scheme I predict Michaelis constants for NADPH and H_2folate close to the experimentally observed values. The increased values of K_m for both substrates compared with wt enzyme are a consequence of the different enzyme complexes with which the substrates combine in the two mechanisms. For wt enzyme operating under conditions of steady state, and saturating substrate concentrations, H_2folate combines primarily with the enzyme·NADP complex and NADPH primarily with the enzyme·H_2folate complex. However, for F31L enzyme under these conditions, H_2folate combines almost exclusively with the enzyme·NADPH complex and NADPH with the enzyme·H_4folate complex. Since NADPH only combines to a significant extent with one enzyme complex, there is only one K_m and not two as in the case of wt enzyme, for which there is significant binding to enzyme·H_4folate as well as to enzyme·H_2folate. The increased K_i for NADP compared with its values for wt enzyme is a function of the lowered k_{on} values for NADP for all forms of F31L with which it combines, together with greatly decreased flux through the E·NADP·H_2folate pathway. H_4folate is inhibitory for F31L because it competes with H_2folate for E·NADPH, which it converts back to the abortive complex. Since H_4folate binds very weakly to wt E·NADPH, this product has no inhibitory effect except at very high concentrations. At moderate concentrations it has an activating effect by competing with H_2folate for E·NADP, which it converts back to the ternary product complex with flux of some of this through the lower fast pathway.

Effect of the Mutation on Pre-Steady-State Kinetics. F31L rHDHFR has a burst reaction followed by decceleration to steady state after a single turnover, which is in contrast to wt enzyme, which exhibits a hysteretic phase between the initial burst and achievement of steady state (Appleman et al., 1989). This is readily interpreted in terms of the different mechanistic behaviors proposed for the two enzymes. In the case of wt enzyme hysteresis occurs as a switch of flux occurs from the lower pathway through E·NADPH·H_4folate to the upper pathway through E·NADP·H_2folate (Appleman et al., 1990). For F31L enzyme flux continues to be primarily through the former pathway, and no hysteresis is observed.

As in the case of wt enzyme, the isotope effect for the burst reaction catalyzed by F31L is small (1.9), an observation indicating that a reaction other than hydride transfer is rate limiting during the burst (Beard et al., 1989). This is postulated to be an isomerization of the ternary substrate complex that must precede or accompany hydride transfer. The calculated rate constant for this isomerization as well as that for hydride transfer is substantially decreased by the mutation. This is presumably an effect of the Phe^{31} → Leu substitution on the precise position of the pteridine ring of the substrate with respect to the nicotinamide ring of bound NADPH. Benkovic et al. (1988) have shown that the rate of hydride transfer is very sensitive to the distance between these rings and their relative orientations.

Overall Effect of the Mutation on Efficiency. Although the effect of the mutation on hydride transfer does not affect the overall rate of catalysis, the decreased rates of dissociation of H_4folate from its complexes do. In order to determine the effect of the mutation on the efficiency of the enzyme, the rate of product formation was computed by use of the CRICF program. The initial concentrations of reactants and products were chosen to match approximately those in a eukaryotic cell: NADPH, 2000 μM; H_2folate, 0.1 μM; NADP, 20 μM; and H_4folate, either 1 or 10 μM. The concentration of enzyme was set at 0.001 μM but does not affect the calculation unless it becomes very high (much greater than 0.1 μM), provided the concentrations of substrates and products are not allowed to change during the time course of the simulation. With 1 μM H_4folate, calculated values for k_{cat} are 6.9 s^{-1} for wt and 2.1 s^{-1} for mutant. With 10 μM H_4folate present, the corresponding values are 5.0 and 0.58 s^{-1}, respectively. Thus, the Phe^{31} → Leu mutation, by increasing H_4folate binding (perhaps by allowing a forbidden conformation change in the E·NADPH·H_4folate complex), significantly impairs enzyme efficiency under physiological conditions.

Comparison of F31L rHDHFR and ECDHFR. The Phe^{31} → Leu mutation makes the hydrophobic cavity of HDHFR structurally more like that of DHFR from *E. coli* and *Lactobacillus casei*. These bacterial DHFRs have an active site very similar to that of HDHFR but have Leu in the position

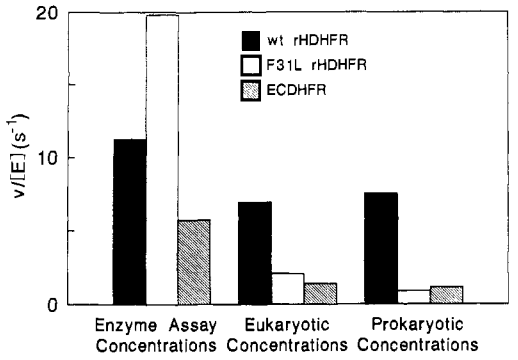

FIGURE 8: Comparison of computed rates of steady-state catalysis by wt rHDHFR, F31L rHDHFR, and ECDHFR at concentrations of substrates and products typical of assay conditions, eukaryotic cell conditions, and parokaryotic cell conditions. See Figure 7 for concentrations used.

corresponding to Phe^{31}. Other amino acid side chains making direct interactions with bound pteridines are identical in the bacterial DHFRs and in HDHFR, except that the bacterial counterpart of Glu^{30} in HDHFR is an Asp. It is therefore of interest to examine whether the $Phe^{31} \rightarrow$ Leu mutation makes HDHFR more like ECDHFR in catalysis and in ligand binding. In some respects the F31L enzyme retains properties like those of wt rHDHFR. Thus, it is very weakly inhibited by trimethoprim (K_i 1.1 μM) like the wt (K_i 1.0 μM) (Prendergast et al., 1989) and in contrast to ECDHFR (K_i 0.08 nM) (Appleman et al., 1988a). Both the human enzymes have an obligatory conformational change involved in the chemical transformation step, and there is no evidence for this with ECDHFR. On the other hand, F31L HDHFR resembles ECDHFR and not wt HDHFR in the use of essentially a single catalytic pathway at steady state, with H_4folate dissociation as the only rate-limiting step except at high pH when hydride transfer becomes rate limiting. As a consequence, the steady-state distribution of F31L enzyme among its complexes in many respects resembles that for ECDHFR more than that for wt rHDHFR (Figure 7). The calculated k_{cat} for F31L rHDHFR also more closely resembles that for ECDHFR at physiological concentrations of substrates and inhibitors (Figure 8). The final point of resemblance between F31L enzyme at ECDHFR is the lack of observable hysteresis between the burst phase and steady state. F31L enzyme has a rate constant for hydride transfer at pH 7.65 (1200 s^{-1}) intermediate between that for wt (3000 s^{-1}) and for ECDHFR (51 s^{-1}). On the other hand, the pH dependence of k_{cat} for F31L is unlike that of either of the other enzymes. Thus, the mutant is more like ECDHFR in some respects, but other important structural differences determine properties of the bacterial enzyme.

ACKNOWLEDGMENTS

We thank Vicki Gray for typing the manuscript.

REFERENCES

Appleman, J. R., Howell, E. E., Kraut, J., Kühl, M., & Blakley, R. L. (1988a) *J. Biol. Chem. 263*, 9187–9198.

Appleman, J. R., Prendergast, N., Delcamp, T. J., Freisheim, J. H., & Blakley, R. L. (1988b) *J. Biol. Chem. 263*, 10304–10313.

Appleman, J. R., Beard, W. A., Delcamp, T. J., Prendergast, N. J., Freisheim, J. H., & Blakley, R. L. (1989) *J. Biol. Chem. 264*, 2625–2633.

Appleman, J. R., Beard, W. A., Delcamp, T. J., Prendergast, N. J., Freisheim, J. H., & Blakley, R. L. (1990) *J. Biol. Chem. 265*, 2740–2748.

Beard, W. A., Appleman, J. R., Delcamp, T. J., Freisheim, J. H., & Blakley, R. L. (1989) *J. Biol. Chem. 264*, 9391–9399.

Benkovic, S. J., Fierke, C. A., & Naylor, A. M. (1988) *Science 239*, 1105–1110.

Birdsall, B., Burgen, A. S. V., & Roberts, G. C. K. (1980) *Biochemistry 19*, 3723–3731.

Cayley, P. J., Dunn, S. M. J., & King, R. W. (1981) *Biochemistry 20*, 874–879.

Chen, J.-T., Mayer, R. J., Fierke, C. A., & Benkovic, S. J. (1985) *J. Cell. Biochem. 29*, 73–82.

Chen, J.-T., Taira, K., Tu, C.-P. D., & Benkovic, S. J. (1987) *Biochemistry 26*, 4093–4100.

Fierke, C. A., Johnson, K. A., and Benkovic, S. J. (1987) *Biochemistry 26*, 4085–4092.

Howell, E. E., Warren, M. S., Booth, C. L. J., Villafranca, J. E., & Kraut, J. (1987) *Biochemistry 26*, 8591–8598.

Mayer, R. J., Chen, J.-T., Taira, K., Fierke, C. A., & Benkovic, S. J. (1986) *Proc. Natl. Acad. Sci. U.S.A. 83*, 7718–7720.

Murphy, D. J., & Benkovic, S. J. (1989) *Biochemistry 28*, 3025–3031.

Oefner, C., D'Arcy, A., & Winkler, F. K. (1988) *Eur. J.* Biochem. *174*, 377–385.

Pfleiderer, W. (1985) in *Folates and Pterins, Vol. 2, Chemistry and Biochemistry of Pterins* (Blakley, R. L., & Benkovic, S. J., Eds.) pp 43–114, John Wiley & Sons, New York.

Prendergast, N. J., Delcamp, T. J., Smith, P. L., & Freisheim, J. H. (1987) *Fed. Proc. Fed. Am. Soc. Exp. Biol. 46*, 2260.

Prendergast, N. J., Delcamp, T. J., Smith, P. L., & Freisheim, J. H. (1988) *Biochemistry 27*, 3664–3671.

Prendergast, N. J., Appleman, J. R., Delcamp, T. J., Blakley, R. L., & Freisheim, J. H. (1989) *Biochemistry 28*, 4645–4650.

Schweitzer, B. I., Srimatkandada, S., Gritsman, H., Sheridan, R., Venkataraghavan, R., & Bertino, J. R. (1989) *J. Biol. Chem. 264*, 20786–20795.

Taira, K., & Benkovic, S. J. (1988) *J. Med. Chem. 31*, 129–137.

Thillet, J., Absil, J., Stone, S. R., & Pictet, R. (1988) *J. Biol. Chem. 263*, 12500–12508.